Journal of Photochemistry and Photobiology A: Chemistry 205 (2009) 186–196

Contents lists available at ScienceDirect

Journal of Photochemistry and Photobiology A: Chemistry

journal homepage: www.elsevier.com/locate/jphotochem

Characterization of guest molecule concentration dependent nanotubes of β-cyclodextrin and their secondary assembly: Study with trans-2-[4(dimethylamino)styryl]benzothiazole, a TICT-fluorescence probe

M. Sowmiya, Pradipta Purkayastha, Amit K. Tiwari, S. Syed Jaffer, Subit K. Saha*

Department of Chemistry, Birla Institute of Technology and Science, Pilani 333031, Rajasthan, India

ARTICLE INFO

Article history:
Received 17 September 2008
Received in revised form 13 March 2009
Accepted 4 May 2009
Available online 12 May 2009

Keywords:
DMASBT
β-Cyclodextrin nanotube
Secondary assembly
TICT fluorescence
Fluorescence anisotropy
Atomic force microscopy
Transmission electron microscopy
Critical aggregation concentration

ABSTRACT

The formation of nanotubes of β-cyclodextrins (β-CD) and their secondary assembly induced by trans-2-[4-(dimethylamino)styryl]benzothiazole (DMASBT) as a guest molecule has been explained using twisted intramolecular charge transfer (TICT) fluorescence, steady state fluorescence anisotropy, time-correlated single-photon counting fluorescence decay of DMASBT, atomic force microscopy and also transmission electron microscopy. It has been demonstrated that although at lower concentration of β-CD, DMASBT molecules form simple adduct of 1:1 stoichiometry but they form extended nanotubes at relatively high concentration of β-CD which further lead to the secondary assembly through intertubular hydrogen bondings forming rod-like structures. The changes in fluorescence properties of DMASBT yield critical aggregation concentration (CAC) of β-CD very close to 2.5 mM. The extent of formation of these supramolecular structures is dependent on the concentration of guest molecule. It has been observed that perchlorate ion (ClO_4^-) reduces the stability of supramolecular structures at higher concentration of it but at low concentration (<7 mM) it enhances the stability by providing the anchor sites for intermolecular hydrogen bonding between neighboring β-CD molecules. The polarity and viscosity dependent TICT fluorescence characteristics of DMASBT are exploited to determine the micropolarity and microviscosity of environment around it inside the nanotubes.

1.. Introduction

Recently, the study of the formation of nanotubes by α-, β- and γ-cyclodextrins (α-CD, β-CD and γ-CD) in presence of some other organic molecules (guest) has become a subject of great interests [1–14]. The formation of other supramolecular assemblies of cyclodextrins such as rotaxanes [15] and polyrotaxanes [16], catenanes [17], supramolecular tape [18] and "molecular necklace" or threaded cyclodextrins [19] is also reported recently and has grown interests for their various applications in the design of molecular devices [20–25]. Depending on the nature of guest and host (cyclodextrins) molecules and the concentration of latter there may be formation of adduct [10–14,24–27] with stoichiometric ratio (guest:CD) 1:1 or 1:2 or formation of nanotubes [1–9]. As for example [4], β-CD forms 1:1 inclusion complex with 2-phenyl-5-(4-diphenylyl)1,3,4-oxadiazole (PBD) at lower concentration and nanotubes at sufficiently higher concentration, γ-CD forms nanotubes, whereas α-CD forms 1:2 (PBD:CD) adduct. PBD and some other oxazole molecules form simple inclusion complexes with γ-CD at lower concentrations and extended nanotubes by these inclusion complexes at relatively high concentrations [6–8]. The dependence of concentration and size of cyclodextrins for the formation of nanotubes is also reported by Wu et al. in case of N,N′-diphenylbenzidine (DPB) as guest molecule [3]. Furthermore, depending on the relative sizes of host and guest molecules, more than one guest molecule can be included in the hydrophobic cavity of cyclodextrins [28,29]. Li and McGown [1] reported the formation of nanotubes by the inclusion of two and three guest molecules per molecule of β-CD and γ-CD, respectively with the partial overlapping arrangement of guest molecules, diphenylhexatriene (DPH) inside the nanotubes. They have suggested that on an average 20 β-CDs or 30 γ-CDs are present per nanotube and have not seen any nanotube formation in case of DPH–α-CD system. For β-CD–PBD and γ-CD–DPB systems mentioned above maximum numbers of cyclodextrin molecules per nanotube are reported to be 27 and 16, respectively. Although Li and McGown [1] noticed nanotubes formation in the aqueous solution of DPH in β-CD, but Pistolis and Malliaris [2] reported simple 1:1 β-CD–DPH adducts in DMF/water mixtures.

The self-aggregations of α-, β- and γ-CDs and some modified CDs in water in absence of any guest molecules have been reported in the literature [30–36]. Cyclodextrins exist as aggregates in solu-

* Corresponding author. Tel.: +91 1596 245073x238; fax: +91 1596 244183.
E-mail addresses: sksaha@bits-pilani.ac.in, subitk_saha@yahoo.com (S.K. Saha).

1010-6030/$ – see front matter © 2009 Elsevier B.V. All rights reserved.
doi:10.1016/j.jphotochem.2009.05.002

tion bound together by a network of hydrogen bonds. Wu et al. [3,4] have reported the secondary aggregation of guest molecule induced nanotubes of β-CD and γ-CDs in aqueous medium. According to them, besides hydrophobic and van der Waals interactions, the hydrogen bonding between the hydroxyl groups of neighboring cyclodextrin molecules is necessary for the formation of the nanotubular structure. The rod-like structure is formed by the secondary assembly of cyclodextrin nanotubes. The driving force for the secondary assembly is mainly inter-nanotubular hydrogen bonding [3,4]. The assembly of cyclodextrin takes place in three dimensions two of which are favored over the third, similar to the construction of wall by the use of bricks, resulting in micrometer-sized rods with variable length and width, but constant thickness [18]. The hydrogen bonding in secondary assembly in solution is explained by Wu et al. [3,4] by the fact that at pH 13.0 when hydroxyl groups of β-CD turn to deprotonated form no rod-like structure except spherical ones are observed by transmission electron microscopy.

Although the effect of concentrations of CDs on the formation of nanotubes has been reported by many groups, but the dependence of nanotube formation on the concentration of guest molecule is rarely reported [37]. In the present work, we have reported the guest molecule concentration dependent extent of formation of nanotubes of β-CD and their secondary assembly with the help of twisted intramolecular charge transfer (TICT) fluorescence characteristics of trans-2-[4-(dimethylamino)styryl]benzothiazole (DMASBT) (Scheme 1) as guest molecule, its steady state fluorescence anisotropy and time-correlated single photon counting (TCSPC) fluorescence decay, atomic force microscopy (AFM) and transmission electron microscopy (TEM) images. Although secondary assembly has been reported by Wu et al. [3,4] but in this work the supramolecular structures formed by the aggregation of rod-like structures are demonstrated by AFM micrographs. Apart from this, the effect of salting-in agent, sodium perchlorate ($NaClO_4$) on the formation of supramolecular structures has also been discussed. It is known that salting-in agent increases the solubility of organic compounds in water [38–40]. Since hydrophobic interaction is a key factor for the formation of inclusion complex between CDs and small guest molecules, increased aqueous solubility of both of them in presence of a salting-in agent has been found to decrease the binding constants of the inclusion complexes [24,41]. It has also been reported in the literature that the effect of low concentration of perchlorate ions, ClO_4^- on the binding constant of the CDs with guest molecule containing polar groups, such as $-NH_2$, –OH is different from that of higher concentration of ClO_4^- ions [24,41]. In this work, we have shown first time the effect of low as well as high concentrations of ClO_4^- ions on the formation of guest molecule induced supramolecular structures and it has been observed that ClO_4^- ions affect similarly even in case of guest molecule containing comparatively nonpolar group, $-N(CH_3)_2$ as it is in the case of DMASBT. Although micropolarity of simple adduct has been reported (discussed later), but first time we have determined the micropolarity and microviscosity of environment around guest molecule inside the nanotubes.

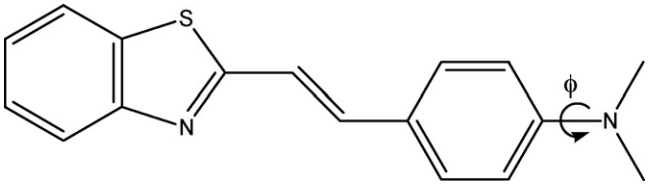

Scheme 1. Molecular structure of DMASBT.

2.. Experimental

2.1. Materials and methods

DMASBT and β-CD were procured from Aldrich Chemical Company, WI, USA. The methods of recrystallization and purity check of DMASBT are mentioned elsewhere [42]. β-CD was used without further purification. Methanol used as solvent is of spectroscopic grade and procured from Spectrochem Chemical Company, India. $NaClO_4$ was supplied by Himedia, India. NaOH and H_2SO_4 used for the adjustment of pH of the solutions were procured from Merck, India. Triple distilled water was used for the preparation of the aqueous solutions. To record the UV–vis absorption and fluorescence spectra of DMASBT in pure solvents, a stock solution of DMASBT (1 mM) was prepared in pure methanol. For the preparation of aqueous solutions of different concentrations of β-CD with constant concentration of DMASBT, 0.05 mL of DMASBT solution in methanol was added to a required volume of aqueous solution of β-CD and the final volume of it was adjusted to 10 mL. Methanol was added due to low solubility of DMASBT in water. The percentage of methanol present in all the solutions is only 0.5. To study the effect of concentrations of DMASBT on the extent of formation of nanotubes, three different concentrations of DMASBT have been chosen: those are 2 μM, 3 μM and 5 μM. To study the effects of ClO_4^- ions on the formation of nanotubes of β-CD the solutions of various concentrations of ClO_4^- ions with same concentrations of DMASBT (2 μM or 3 μM or 5 μM) and β-CD (10 mM) are prepared for which required volume of aqueous solution of $NaClO_4$ is added to the solutions of DMASBT and β-CD. All experimental solutions were adjusted to a pH value of 7.4. The fluorescence quantum yields were determined with respect to that of quinine sulfate in 0.1N H_2SO_4 as 0.55 and calculating the area under the fluorescence bands of both DMASBT and quinine sulfate.

The absorption spectra were recorded using a Jasco V570 UV–vis spectrophotometer. Fluorescence measurements were performed using a Shimadzu RF-5301PC scanning spectrofluorimeter. Fluorescence lifetimes were determined from time-resolved intensity decay by the method of time-correlated single-photon counting using a picosecond diode laser at 370 nm (IBH, U.K., nanoLED-07) as light source. The typical response time of this laser system was 50 ps. The fluorescence decays were deconvoluted using IBH DAS6 software.

The steady state fluorescence anisotropy measurements were performed with the same steady state spectrofluorimeter fitted with a polarizer attachment. The excitation and emission bandwidths used for the anisotropy measurements were 5 nm each. The steady state anisotropy, r can be represented as [43]:

$$r = \frac{I_{VV} - GI_{VH}}{I_{VV} + 2GI_{VH}} \quad (1)$$

where I_{VH} and I_{VV} are the intensities obtained from the excitation polarizer oriented vertically and the emission polarizer oriented in horizontal and vertical positions, respectively. The factor G is defined as

$$G = \frac{I_{HV}}{I_{HH}} \quad (2)$$

where I terms refer to parameters same as mentioned above for the horizontal position of the excitation polarizer. All measurements were carried out at room temperature (25 °C). The AFM experiments were done using a Nanoscope II instrument (Digital Instrument Inc., USA) with lateral resolution of 1 Å and vertical resolution of 0.1 Å. The substrate used for AFM as HOPG (highly organized pyrolytic graphite). TEM micrographs were recorded with a Hitachi H7500 instrument. One tiny drop of the solution of sample was placed onto a carbon coated gold grid.

3.. Results and discussion

3.1. UV–vis absorption spectra

The absorption spectrum of DMASBT changes with varying concentration of β-CD. With increasing concentration of β-CD absorption band gets blue shifted. Although no proper isosbestic point is found but absorbance values are close to a constant value at ~370 nm (see supporting information). Change of absorption spectra with changing the concentration of β-CD supporting the binding of DMASBT with β-CD; but unavailability of proper isosbestic point is due to the fact that with changing the concentration of β-CD, solution consists of mixture of nanotubes of different lengths as discussed later. The absorption spectra of DMASBT are much less sensitive to the varying concentration of β-CD than fluorescence spectra.

3.2. Steady state fluorescence characteristics of DMASBT in β-CD

The changes of fluorescence spectra with changing the concentrations of β-CD associated with DMASBT of concentration 5 μM are shown in Fig. 1. The fluorescence band maxima gets blue shifted by 11 nm in 10 mM β-CD compared to the band maxima in aqueous medium. It has been shown earlier [42] that DMASBT undergoes normal as well as highly Stokes shifted fluorescence. While normal fluorescence takes place from the locally excited (LE) state, the twisted intramolecular charge transfer (TICT) state is responsible for highly Stokes shifted fluorescence. The theoretical calculations have suggested that the large stabilization of third excited singlet state, S_3 of DMASBT with twisted conformation (torsion angle, $\phi = 90^\circ$, Scheme 1) of electron donor, $-N(CH_3)_2$ group with respect to electron acceptor styrylbenzothiazole group in polar environments is responsible for highly Stokes shifted charge transfer fluorescence [42,44]. Initially the appearance of broad structureless Stokes shifted fluorescence bands in polar solvents and dependence of the fluorescence quantum yields on the polarity of the solvents suggested the charge transfer (CT) character of the emitting state in polar media. Later, detailed fluorescence study in the medium of varying polarities have shown that actually TICT fluorescence quantum yield increases, reaches maximum and then decreases in a medium of very high polarity [42,45]. In a highly polar medium due to the greater stabilization of the TICT state, the nonradiative processes become faster as a result of the closer proximity of TICT state towards triplet as well as S_0^{TICT} states [42,45,46]. With decreasing the polarity of the medium, the TICT fluorescence quantum yield increases with the blue shift of fluorescence due to the concomitant increase in the energy gap between S_3^{TICT} and S_0^{TICT} states as well as triplet state [42,47]. Therefore, the above-mentioned increase in fluorescence intensity with blue shift of fluorescence band as a result of increasing concentration of β-CD suggests the transfer of DMASBT molecules from the polar bulk aqueous medium to the nonpolar hydrophobic pocket provided by β-CD molecules [24,41]. The change of fluorescence band maxima with changing the concentration of β-CD with 5 μM DMASBT is shown in Fig. 1(inset). The steady state fluorescence study is also done with the lower concentrations of DMASBT (2 μM and 3 μM) in various concentrations of β-CD. Similar to the study with high concentration of DMASBT in these cases also the blue shift of fluorescence bands with increase in fluorescence quantum yield with increasing concentration of β-CD is observed (figure not shown). However, surprisingly the increase of fluorescence quantum yield is greater with higher concentration of DMASBT at the same concentration of β-CD. To compare this, the ratios, I/I_o (where I and I_o are intensities with and without β-CD, respectively) and fluorescence quantum yields in cases of low (2 μM and 3 μM) and high (5 μM) concentrations of DMASBT have been plotted against the concentration of β-CD in Fig. 2 and (inset), respectively. The sigmoid fittings have been done up to 10 mM concentration of β-CD in cases of 2 μM and 3 μM of DMASBT, whereas in case of 5 μM of DMASBT it is done only up to 9 mM of β-CD. These figures are in support to the fact that the change in fluorescence quantum yields with changing the concentration of β-CD depends on the concentration of guest molecule, DMASBT. The decrease of fluorescence intensity ratio as well as fluorescence quantum yield above ~9 mM concentration of β-CD should be noted which will be discussed later. While the increase in quantum yield in 9 mM β-CD is 11 times with 5 μM of DMASBT, the same is only 4.7 times and 4 times with 3 μM and 2 μM of DMASBT, respectively relative to the quantum yield in aqueous medium. The increases in fluorescence intensity at the same concentration of β-CD are 6, 3.8 and 3.5 times relative to the intensity in aqueous solution with 5 μM, 3 μM and 2 μM of DMASBT, respectively. This dissimilarity in the enhancement of fluorescence quantum yields due to the inclusion of DMASBT molecules inside the β-CD cavities suggests that envi-

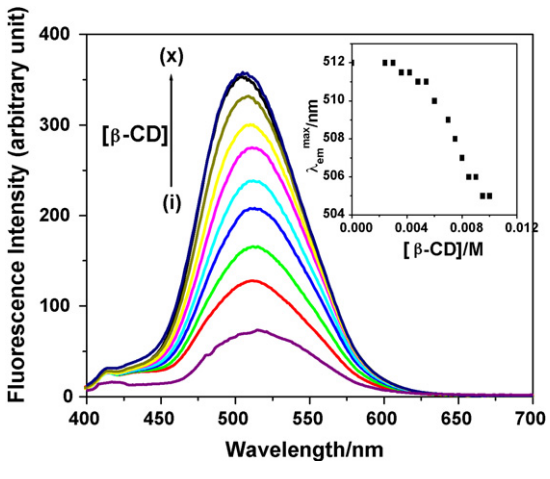

Fig. 1. Fluorescence spectra of DMASBT (5 μM) as a function of concentration of β-CD (λ_{ex} = 370 nm). Spectra $i \rightarrow x$ correspond to 0(▬), 2.4(▬), 3.0(▬), 3.6(▬), 4.2(▬), 4.8(▬), 5.4(▬), 7.0(▬), 7.5(▬) and 10(▬) mM β-CD, respectively. [Inset represents fluorescence peak maxima of DMASBT (5 μM) as a function of concentration of β-CD (λ_{ex} = 370 nm)].

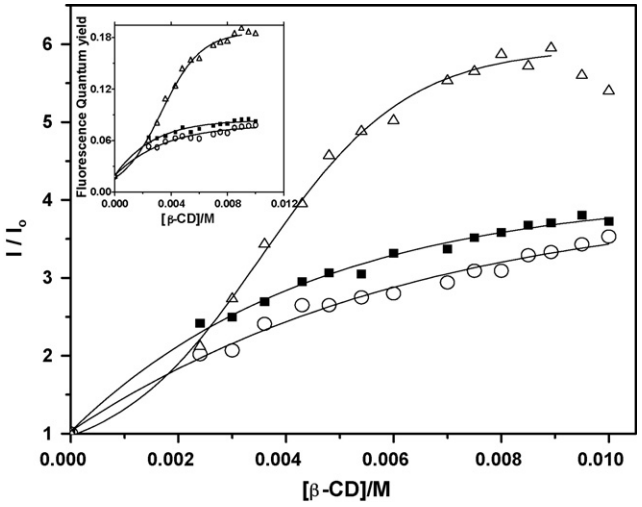

Fig. 2. Plot of fluorescence intensity ratios of DMASBT as a function of concentration of β-CD (λ_{ex} = 370 nm, λ_{em} = 515 nm). [Inset shows fluorescence quantum yields of DMASBT as a function of concentration of β-CD (λ_{ex} = 370 nm)]. ((◯), (■) and (△) are for 2 μM, 3 μM and 5 μM DMASBT, respectively).

ronments around the guest molecules in β-CD are different with different concentrations of DMASBT.

3.3. Study of fluorescence anisotropy

The fluorescence anisotropy measurement has a great importance due of its potential applications in the field of biochemical research because the observed anisotropy will be affected by a factor which affects shape, size, segmental flexibility or rotational motion of a molecule [43]. The fluorescence anisotropy can be increased as a result of an increase in the rigidity of the surrounding of a fluorophore [43]. Therefore, the extent of restriction imposed by the microenvironment on the dynamic properties of DMASBT can be reflected by the fluorescence anisotropy which can be exploited for finding out the probable location of DMASBT in the microheterogeneous environment such as β-CD [43,48,49]. The plots of variation of fluorescence anisotropy of DMASBT as a function of concentration of β-CD are shown in Fig. 3 in presence of various concentrations of DMASBT in β-CD. The sigmoid fittings have been done up to 8 mM concentration of β-CD. It can be seen that in all the cases there are huge enhancement of fluorescence anisotropy with increasing concentration of β-CD. This can be attributed to the significant restriction of rotational diffusion of the molecule and can be correlated with the increase in fluorescence quantum yield. The continuous increase of fluorescence anisotropy with the addition of β-CD and a very high value of fluorescence anisotropy is in support of the formation of nanotubes of β-CD induced by DMASBT. As mentioned above formations of nanotubes by cyclodextrins in solution phase have been explained by many groups on the basis of observation of large degrees of fluorescence anisotropies of guest molecules in cyclodextrins [1–4]. The sharp increase in anisotropy for low as well as high concentrations of DMASBT above 2.5 mM concentration of β-CD might be indicating the optimum concentration of β-CD to form nanotubes. The substantial changes in other fluorescence parameters such as fluorescence peak maxima (Fig. 1(inset)), fluorescence intensity (Fig. 2), and quantum yield (Fig. 2(inset)) are also observed only above this concentration (2.5 mM) of β-CD. These changes in fluorescence properties due to aggregation of DMASBT filled β-CD yield the critical aggregation concentration (CAC) very close to 2.5 mM.

To check the association behavior (stoichiometric ratio 1:1 or 2:1) of DMASBT to β-CD and to determine the association constant the data obtained from fluorescence study has been used for Benesi–Hildebrand [24,41,50] plot. The following equations (Eqs. (3) and (4)) were used for 1:1 and 2:1 β-CD–DMASBT association, respectively:

$$\frac{1}{F - F_o} = \frac{1}{F_m - F_o} + \frac{1}{K[\mathrm{CD}]_o(F_m - F_o)} \quad (3)$$

$$\frac{1}{F - F_o} = \frac{1}{F_m - F_o} + \frac{1}{K'[\mathrm{CD}]_o^2(F_m - F_o)} \quad (4)$$

where F_o and F are the fluorescence intensities in the absence and presence of β-CD, respectively, F_m is the limiting intensity of fluorescence, K represents association constant and $[\mathrm{CD}]_o$ is the analytical concentration of β-CD. The apparent K values were determined from the slope and intercept of the Benesi–Hildebrand plots. The excitation wavelength in case of measurement of association constant was 370 nm.

Although nanotubes are formed above 2.5 mM concentration of β-CD, but it has been observed that β-CD at its low concentration (<2.5 mM) forms simple adducts with high as well as low concentrations of DMASBT with stoichiometric ratio 1:1. The fluorescence data nicely correlates with the Benesi–Hildebrand plots for 1:1 complex. The Benesi–Hildebrand plot (regression coefficient = 0.999) for the binding of 5 μM DMASBT with low concentration of β-CD is represented by Fig. 4. The association constants for the inclusion complexes of β-CD are found to be $1228 \pm 25\ \mathrm{M}^{-1}$, $1205 \pm 25\ \mathrm{M}^{-1}$ and $1200 \pm 25\ \mathrm{M}^{-1}$ with 5 μM, 3 μM and 2 μM concentrations of DMASBT, respectively. Wu et al. [4] also noticed 1:1 inclusion complex formation in case of PBD as guest molecule. The complexation of the DMASBT with higher concentration of β-CD is quite different because at higher concentration the sharp increase in the fluorescence anisotropy (Fig. 3) of DMASBT concluded the formation of nanotubes. The Benesi–Hildebrand double reciprocal plot does not show linearity (figure not shown) for 1:1 as well as 1:2 complexation at higher concentration of β-CD is in support to the formation of nanotubes in solution. The Benesi–Hildebrand plot approximation cannot be applied in this case because there are many steps in the nanotube formation [2].

Similar to the fluorescence quantum yield, the increase in fluorescence anisotropy in case of high concentration of DMASBT is much greater than that in case of a lower concentration of DMASBT. When there is a 5 times increase in the fluorescence anisotropy value in 10 mM β-CD relative to the same in water with 5 μM concentration of DMASBT, the same is 4 times in presence of 2 μM concentration of the same molecule (Fig. 3). The fluorescence anisotropy of 5 μM DMASBT in 10 mM β-CD is found to be 0.32 which is close to the value (0.321) observed by Li and McGown [1] for DPH in the nanotubes of β-CD. Therefore, the greater extent of increase in fluorescence quantum yield as well as fluorescence anisotropy for the binding of high concentration of DMASBT with β-

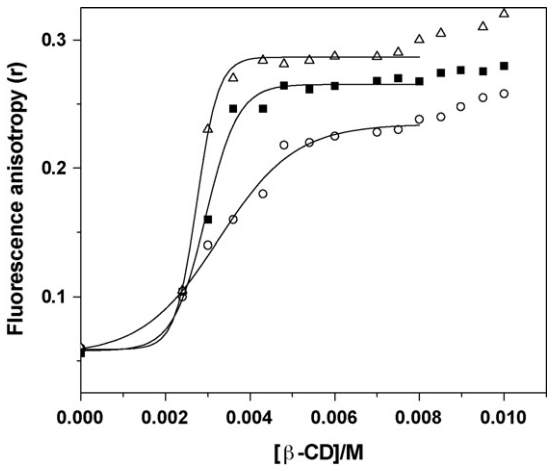

Fig. 3. Plot of steady state fluorescence anisotropy of DMASBT as a function of concentration of β-CD (λ_{ex} = 370 nm, λ_{em} = 515 nm). ((○), (■) and (△) are for 2 μM, 3 μM and 5 μM DMASBT, respectively).

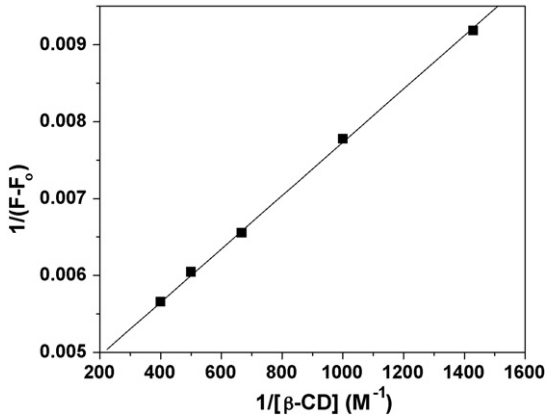

Fig. 4. Benesi–Hildebrand plot for DMASBT (5 μM) in β-CD.

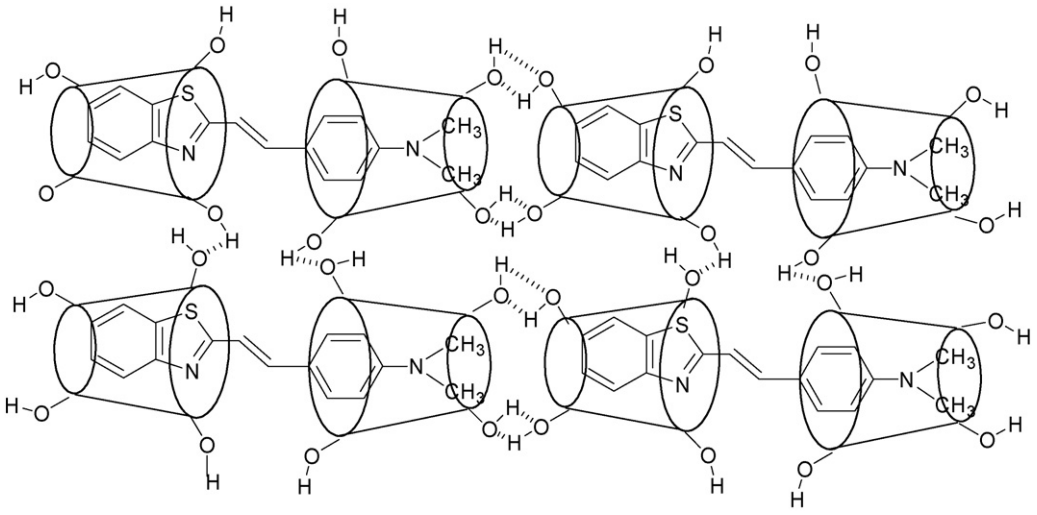

Scheme 2. Structure of nanotubes and their secondary assembly.

CD suggests that the extent of formation of nanotubes is induced by the concentration of guest molecules. As explained later there are not only the formations of nanotubes but also secondary assembly of nanotubes as well (Scheme 2). The secondary assembly of nanotubes of β-CD and γ-CD induced by PBD and DPB as guest molecule, respectively are also reported by Wu et al. [3,4]. Our observation suggests that although nanotubes are formed with low as well as high concentration of DMASBT, but the degree of secondary assembly of nanotubes also depends on the concentration of DMASBT. The microenvironment around DMASBT is different when the formation of nanotubes is induced by high concentration of it compared to the low concentration. The decrease in fluorescence intensity ratio and therefore fluorescence quantum yield observed at higher concentration (>9 mM) of β-CD with 5 μM of DMASBT (Fig. 2 and inset) is due to the scattering of lights caused by high degree of assembly. This decrease was not visible in case of lower concentration of DMASBT. This also supports lower extent of formations of nanotubes and their assembly with low concentration of guest molecules. The scatterings of lights by nanotubes are also observed by many other groups [1,3,4]. Therefore, it can be stated that in order to form nanotubes, presence of guest molecules is must and the morphologies of aggregation of nanotubes are dependent on the concentration of guest molecules. This further suggests that inclusion complex formation and their extension to build nanotubes are induced by hydrophobic interactions between β-CD molecules and guest molecules. In comparison to the secondary aggregation of mostly empty nanotubes of β-CD induced by PBD as reported by Wu et al. [4], we would suggest in this case the aggregation of nanotubes filled with DMASBT only; otherwise, low values of fluorescence anisotropy and quantum yield of guest molecule would have been observed if all of them would have come out of the tubes. Moreover, high values of fluorescence properties with higher concentration of DMASBT compared to that with lower concentration of the same are also in support to this fact.

3.4. Images from AFM and TEM

The side view of AFM images of nanotubes of β-CD and their self-aggregation induced by the high concentration (5 μM) of DMASBT can be seen in Fig. 5a. The upper view of the same is represented by Fig. 5b. The rod-like structure represented by an arrow in Fig. 5a is formed due to the secondary assembly of a number of nanotubes. The lengths of such rods are approximately in the range of 150–300 nm. The secondary assembly of nanotubes of β-CD forming rod-like structure reported by Wu et al. [4] had dimension in the range of 500–3000 nm. By these images first time we report the aggregation of a large number of such rods formed by self-assembly of nanotubes of β-CD and also their arrangements with a regular fashion. One can see in Fig. 5a almost parallel rows of aggregations of many rods. The approximate width of a rod will be in between 15 nm and 20 nm. Assuming this width as the length of a nanotube and considering some gap between each pair of β-CD molecules in a tube, there will be approximately 15–20 β-CD molecules per nanotube, because the height of a β-CD molecule is 0.78 nm [51]. In this regard it can be mentioned here that Li and McGown [1] found β-CD–DPH nanotubes containing 20 β-CDs and Wu et al. [4] reported β-CD–PBD nanotubes involving 27 β-CD units in a single nanotube. This image is for 5 μM of DMASBT dissolved in 9 mM β-CD. However, the extent of aggregation of rods is much smaller when low concentration (2 μM) of DMASBT is used as shown in Fig. 5c which suggests that formation of nanotubes and their self-assembly are controlled by the concentration of guest molecule. TEM micrographs of rod-like structure formed by the nanotubes of β-CD (9 mM) with 5 μM and 2 μM of DMASBT are shown in Fig. 6a and b, respectively. The closer view of surface morphology of rod-like structure in case of 5 μM DMASBT–9 mM β-CD system is represented by Fig. 6c. From these figures also one can conclude that the extent of aggregation is more with high concentration of guest molecules than that with lower concentration of the same. A TEM micrograph in case of very low concentration of β-CD (2 mM) with 5 μM of DMASBT is shown in Fig. 6d. Here one can find neither the formation of nanotubes nor their secondary assembly except the formation of only simple adducts. It is worth mentioning that although AFM and TEM images are obtained from solution on solid surface but formation of supramolecular structures, i.e. nanotubes and their secondary assembly are also expected in the solution phase supporting the fact that the high values of fluorescence anisotropy, fluorescence quantum yield and scattering of lights were observed for DMASBT in solution phase only. Moreover, since hydrogen bonding is the driving force for the secondary assembly (Scheme 2) therefore it is expected that rod-like structure can also be formed in the solution phase. In addition to this as mentioned above Benesi–Hildebrand plot did not show any linear relationship for 1:1 as well as 1:2 complexations at higher concentration of β-CD also suggesting nanotube formation in solution phase. However, there is a possibility that morphologies obtained

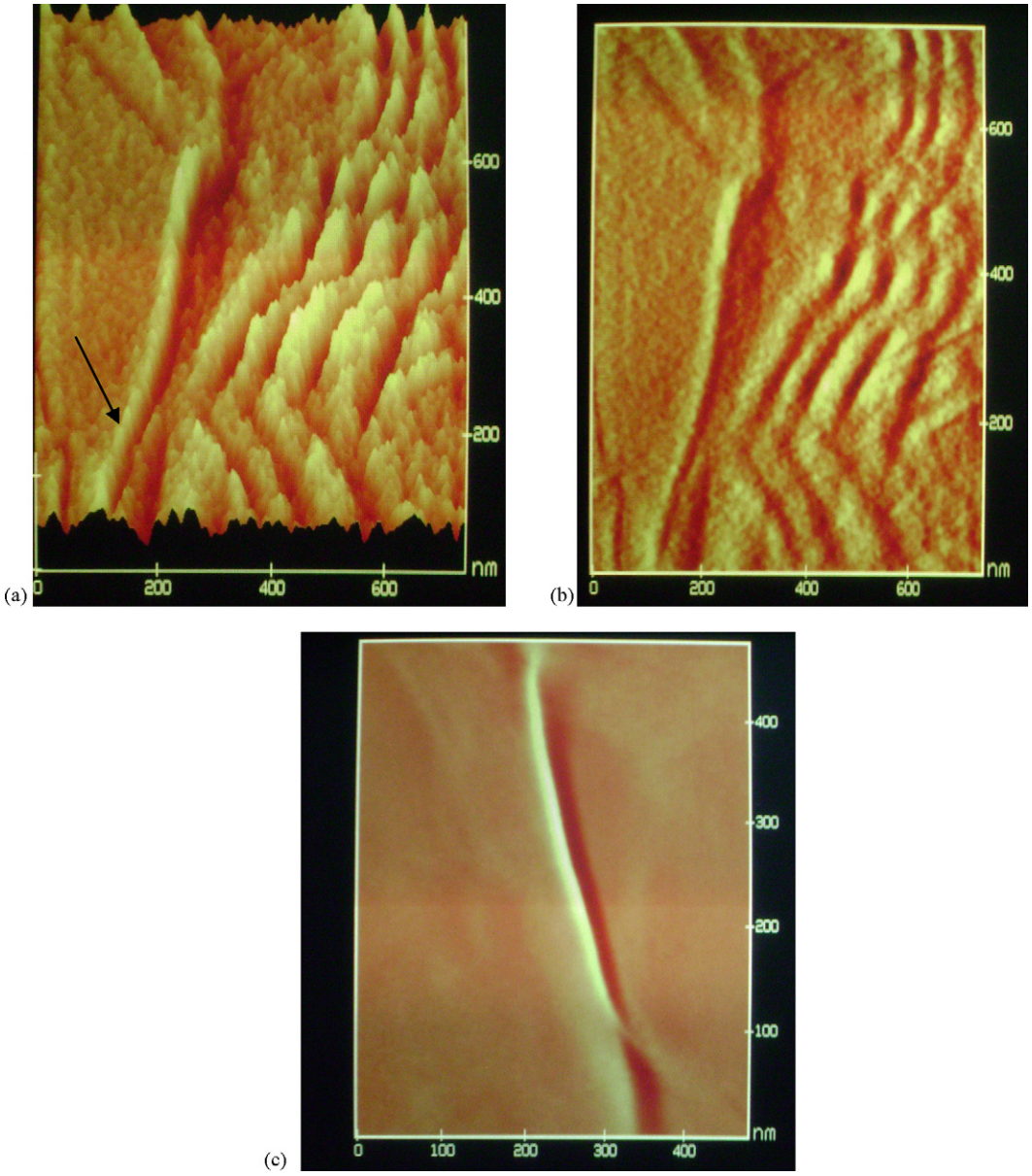

Fig. 5. AFM micrographs for DMASBT–β-CD systems (a) side view, (b) upper view; for both (a) and (b), [DMASBT] = 5 μM and [β-CD] = 9 mM; (c) upper view when [DMASBT] = 2 μM and [β-CD] = 9 mM.

from AFM and TEM images may not be exactly same as that in the solution phase.

3.5. *Effect of sodium perchlorate on nanotube formation*

The increase of hydrocarbon solubility in water in the presence of salting-in reagents (e.g. $NaClO_4$, urea, etc.) is a well known phenomena [38–40]. The decrease in binding constant of guest molecules with β-CDs in presence of salting-in reagents is reported in the literature [24,41]. If hydrophobic interactions play a role in the adduct formation then it is expected that greater water solubility of both guest and host molecules in presence of a salting-in agent will reduce the association between them. Since nanotubes are supramolecular assembly of inclusion complexes, therefore expecting some effects of salting-in agent on the formation of nanotubes, fluorescence anisotropies of DMASBT in 10 mM β-CD with different concentrations of sodium perchlorate (0–0.2 M) have been calculated and plotted in Fig. 7. This figure shows that initially there is a small increase in anisotropy (up to $[ClO_4^-] = 7.0$ mM) which then decreases and remains almost constant up to $[ClO_4^-] = 0.1$ M after that it follows a sharp decrease. It can be mentioned here that among various steps in the mechanism of binding of guest molecule with β-CD, the most important step is to break down the water structure bonded with polar groups such as $-NH_2$ or $-OH$ or $-N(CH_3)_2$ of guest molecule and also the water structure around the aromatic ring [24,41]. Therefore, perchlorate ions, ClO_4^- at moderately high concentration break the water structure, which results in the increase in the water solubility of both DMASBT and β-CD molecules (salting-in effect). The decrease in anisotropy is in accordance with the increase in water solubility which supports the fact that hydrophobic interactions between guest and host is an essential factor for their binding as well as for nanotube formation. However, initial increase in the anisotropy is explained by the fact that perchlorate ions help β-CD molecules to form intermolecular hydrogen bonds between them which favors stronger binding of DMASBT molecules with the β-CD molecules resulting in an increase in anisotropy value. Increase in association constant for the binding of guest molecule with β-CD molecule with

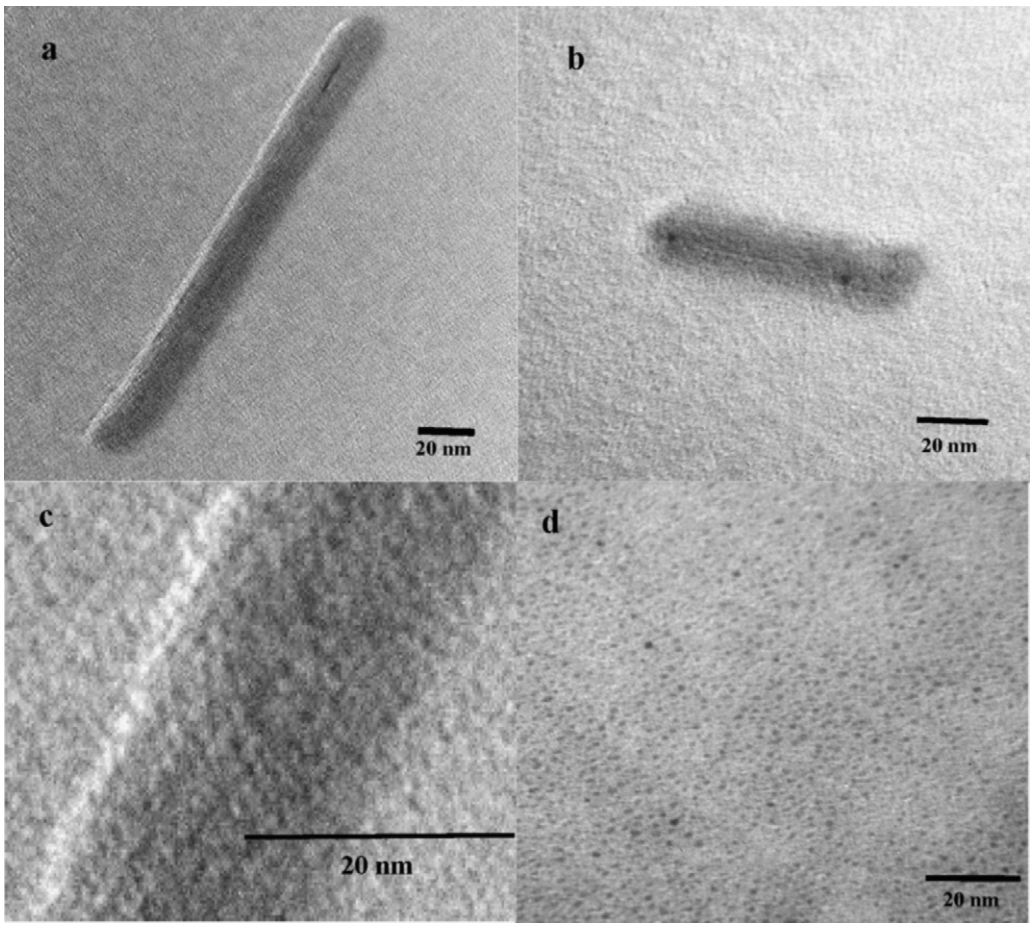

Fig. 6. TEM micrographs of rod-like structures for (a) 9 mM β-CD and 5 μM DMASBT and (b) 9 mM β-CD and 2 μM DMASBT systems. TEM micrographs of (c) closer view of surface morphology of rod-like structure of 9 mM β-CD–5 μM DMASBT system and (d) simple adducts of 2 mM β-CD–5 μM DMASBT system.

low concentration of ClO_4^- ions is demonstrated in the literature [24,41] on the basis of ternary complex formation between a guest molecule containing $–NH_2$ group, a β-CD and a perchlorate ion. In the present study, instead of ternary complex formation a ClO_4^- ion provides an anchor site to two neighboring β-CDs through hydrogen bonds, because DMASBT is having a nonpolar $–N(CH_3)_2$ group. Moreover, a DMASBT molecule is encapsulated by two β-CDs from both sides of it. But at higher concentration of perchlorate ions binding becomes difficult due to the dominating salting-in effect as well as competition between ClO_4^- ions and DMASBT molecules for binding with β-CD molecules [24,41,52]. To support this phenomena, fluorescence intensities and band maxima of DMASBT in 10 mM β-CD are plotted against perchlorate ion concentration in Fig. 8 and inset, respectively. The substantial red shift in fluorescence band maxima and decrease in fluorescence intensity with

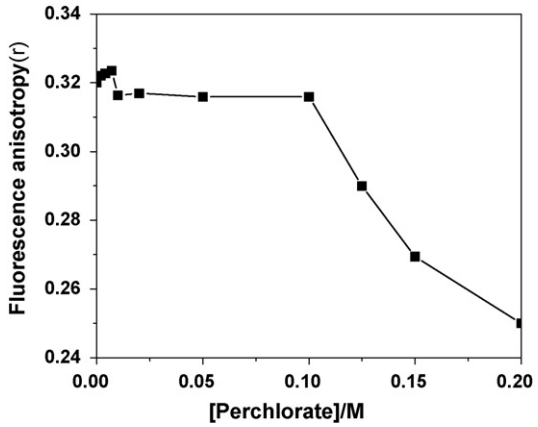

Fig. 7. Variation of steady state fluorescence anisotropy of DMASBT (5 μM) in β-CD (10 mM) with increasing concentration of $NaClO_4$ (λ_{ex} = 435 nm and λ_{em} = 527 nm).

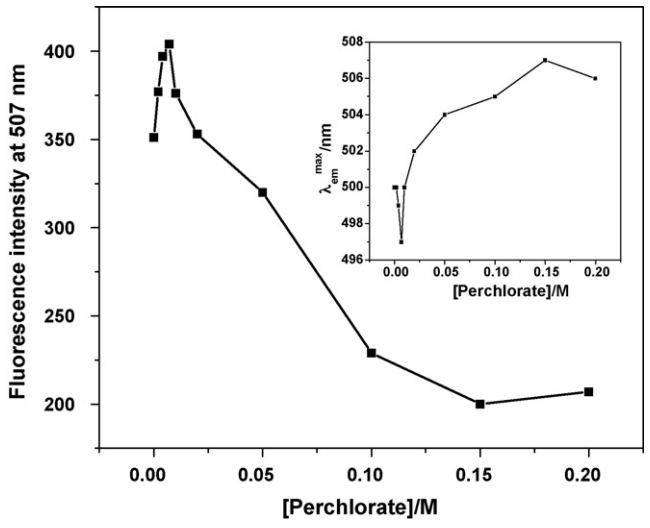

Fig. 8. Plot of fluorescence intensity of DMASBT (5 μM) at 507 nm in β-CD (10 mM) as a function of concentration of $NaClO_4$ (λ_{ex} = 370 nm). [Inset represents the plot of fluorescence peak maxima of DMASBT (5 μM) in β-CD (10 mM) as a function of concentration of $NaClO_4$ (λ_{ex} = 370 nm)].

increasing perchlorate ions concentration above 7.0 mM are as a result of reduced hydrophobic interactions between DMASBT and β-CD molecules thereby increasing the solubility of DMASBT in water and also due to the competition between ClO_4^- ions and DMASBT for binding with β-CD. However, blue shift in fluorescence band maxima and increase in fluorescence intensity at low concentration range (<7.0 mM) of ClO_4^- ions suggest the stronger binding of DMASBT molecules with β-CD as explained above due to the anchoring of ClO_4^- ions and thereby larger stability of nanotubes by the help of ClO_4^- ions. It can be mentioned here that small increase in anisotropy is also observed in the same concentration range of ClO_4^- ions supporting the same fact. This observation insists us to assume that nanotubes may not be stable in this high concentration range of ClO_4^- ions because of two reasons: (i) greater aqueous solubility of both β-CD and DMASBT and (ii) reduced hydrophobic interactions between β-CD and DMASBT. It is now a well known phenomenon that hydrophobic and van der Waals interactions as well as hydrogen bonding interactions are all required for inclusion complexation and formation of extended nanotubes [3,4,24,41]. It can be further suggested that besides hydrophobic, dipole–dipole and hydrogen bonding interactions between host and guest molecules [53,54], hydrogen bonding between –OH groups of neighboring β-CD molecules (Scheme 2) are also essential for the formation of nanotubes of β-CD molecules [4]. Perchlorate ions, at its high concentration break the water structure, which results in the increase in the water solubility of both DMASBT and β-CD molecules (salting-in effect).

3.6. Micropolarity and microviscosity

Having influenced by the high sensitivity of TICT fluorescence of DMASBT towards polarity and viscosity of the environment observed in our recent study [42,45], we have attempted to determine the micropolarity and microviscosity of the environment around guest molecules inside the nanotubes as we have recently determined the same for micelles [55]. The micropolarity is expressed in equivalent scale of $E_T(30)$ which is an empirical solvent polarity parameter comparing the fluorescence behavior of probe molecule in microheterogeneous systems to that in a mixture of homogeneous solvents of varying composition [47,48,56,57]. As referred by Kasha this is static polarity [58]. The Stokes shifts of DMASBT in different compositions of dioxane–water mixtures have been calculated earlier [42] and plotted against $E_T(30)$ (Fig. 9) based on the energy of transition for the solvatochromic intramolecular charge-transfer absorption of the betaine dye 2,6-diphenyl-4(2,4,6 triphenyl-1-pyridono)phenolate as developed by Reichardt [59,60]. Using this plot and the Stokes shift value of 5 μM of DMASBT in 10 mM β-CD, i.e. 5348 cm^{-1} (absorption band maxima = 397 nm, and fluorescence band maxima = 504 nm), the $E_T(30)$ value is coming out to be 54.5 kcal mol^{-1} which is similar to a medium of polarity in between ethanol and methanol [42] that is matching with micropolarity suggested by Heredia et al. [61] and also other group [62]. According to them micropolarity of β-CD cavity is similar to neat methanol. The above-mentioned discussion indicates that the micropolarity of the environment around DMASBT inside the β-CD nanotubes is 54.5. Similarly, the Stokes shift of low concentration (2 μM) of DMASBT in the same concentration of β-CD is calculated to be 5475 cm^{-1} (absorption band maxima = 395 nm, and fluorescence band maxima = 504 nm) which can be correlated with the $E_T(30)$ value equal to 56.3 kcal mol^{-1} that is very close to the $E_T(30)$ of glycerol [42]. The different values of micropolarities and the Stokes shifts in the same concentration of β-CD but with different concentrations of DMASBT also suggest that later is present in two different kinds of environments in β-CD. This is also consistent with the fact that extent of formation of nanotubes and their aggregation is dependent on the concentration of guest molecules. It is worth noting that micropolarity similar to cyclohexane reported by Yang and Bohne [63] in case of binding of pyrene with β-CD is due to the fact that pyrene is completely protected from water unlike quite open structure of complex of DMASBT with β-CD due to difference in structures between DMASBT and pyrene. Moreover, pyrene being more hydrophobic compared to DMASBT is expected to be in a microenvironment less polar than that in case of DMASBT. It should be mentioned here that the fluorescence of DMASBT gets red shifted with increasing percentage of glycerol in glycerol–methanol mixture (spectra not shown here). Fluorescence band is red shifted by 9 nm in pure glycerol compared that in pure methanol. This experiment is done to check the effect of viscosity alone owing to the fact that polarity of glycerol is almost similar to that of methanol. The microviscosity of environment around 5 μM DMASBT in 10 mM β-CD is similar to approximately 80% glycerol–water mixture (discussed later). Although in this viscosity fluorescence spectrum is expected to be red shifted but actually it is blue shifted by 11 nm. This suggests that the effect of polarity is much larger than the effect of viscosity on the fluorescence spectra. If opposite effect (polarity versus viscosity) is comparable then one should not expect much shift in fluorescence band maxima. It should further be stated here that although microviscosity around DMASBT in β-CD cavity is high but due to low polarity (polarity in between ethanol and methanol) and as discussed above greater sensitivity of fluorescence towards polarity bands get blue shifted in presence of β-CD. Since found micropolarity values are in accordance with the fact, it favors the method of determination of micropolarity followed in this work [47,48].

Since fluorescence anisotropy of a fluorescent probe molecule is intimately connected with the viscosity of the microenvironment around it, microviscosity is often estimated from a comparison of the fluorescence anisotropy of a fluorescent probe in an environment with those of the probe in different environments of known viscosities [48,49,64,65]. With a similar intention, we have attempted the fluorescence anisotropy measurements of DMASBT in different percentages (w/w) of glycerol in glycerol–water mixtures [45] (Fig. 9(inset)) and compared the values with the anisotropy values of DMASBT in the nanotubes of β-CD. The fluorescence anisotropies of 5 μM and 2 μM of DMASBT in 9 mM β-CD solution are estimated to be 0.31 and 0.25, respectively (Fig. 3). Comparing these anisotropies with the anisotropies of DMASBT in the glycerol–water mixtures of different viscosities [45], the micro-

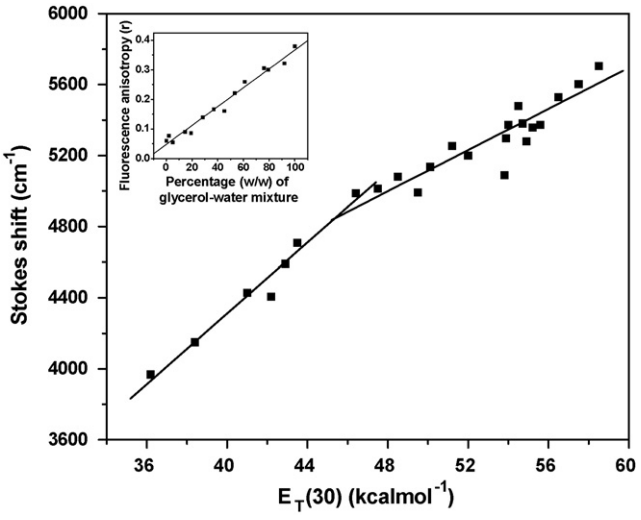

Fig. 9. Variation of Stokes shift of DMASBT (5 μM) in dioxane–water mixture against $E_T(30)$. [Inset represents variation of fluorescence anisotropy (λ_{em} = 550 nm) of DMASBT (1×10^{-5} M) as function of the composition (w/w) of the glycerol–water mixture, λ_{ex} = 367 nm].

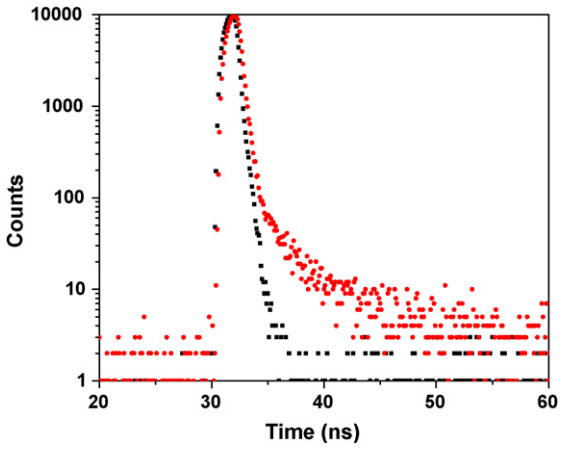

Fig. 10. Fluorescence decay profile (♦) of DMASBT (5 μM) in 9 mM β-CD (λ_{ex} = 370 nm, λ_{em} = 515 nm, and (■) lamp profile).

viscosities of the environments in which DMASBT molecules are residing inside the nanotubes are estimated to be 68 cP and 13 cP for 5 μM and 2 μM of DMASBT, respectively. Those are the viscosities similar to 82/18 (w/w) and 64/36 (w/w) glycerol/water mixture, respectively which again rationalizes that the guest molecules are at different environments. However, these microviscosity values for 9 mM β-CD may be little approximate because of scattering of light during anisotropy measurement although scattering is visible only above 9 mM. But the trend with increasing concentration of DMASBT is expected to be correct. Looking at these microviscosity values one can predict that DMASBT is expected to be moving freely inside the nanotube. Moreover, the successful correlation between the anisotropy in β-CD and in glycerol–water mixture indicates that no additional restriction is imposed on the motion of the overall molecule or the molecule is not trapped in some motionally constrained site due to some specific interactions such as hydrogen bonding between DMASBT and β-CD molecules [49]. This can be rationalized by the fact that $-N(CH_3)_2$ group of DMASBT is incapable of forming hydrogen bonds with β-CD molecules.

3.7. Time-resolved fluorescence study

Fluorescence lifetime data helps to discuss about the local environment around fluorophore [66,67], different interactions involved at the excited state [42,49] and also the solvent relaxations around a fluorophore [68]. Excited singlet state lifetimes of DMASBT could not be determined in most of the solvents because of its very fast decay which was beyond the limitation of our instrument [42]. The lifetimes of DMASBT in β-CD in the concentration range to form nanotubes are also found to be very low but greater than that in conventional solvents. The lifetime values of DMASBT with χ^2 in three different concentrations of β-CD are listed in Table 1. The decay profile of DMASBT in 9 mM β-CD is shown in Fig. 10 as a representative one. The single exponential fittings with lifetimes greater than that in aqueous medium in this concentration range suggest the binding of all molecules of DMASBT with the β-CD molecules. Lifetime increases with increasing the concentration of β-CD which was also noticed in case of binding with the micelles [55]. Therefore, with increasing the concentration of β-CD molecules, there are blue shifts in fluorescence peak maxima, increase in fluorescence quantum yields, fluorescence anisotropy and excited singlet state lifetimes. All these observations rationalize that DMASBT molecules are being transferred to more and more hydrophobic binding sites of β-CD with increasing concentration of it.

The reduced polarity around the probe inside the nanotubes with increasing concentration of β-CD is now reflected in the increase in fluorescence lifetime. The radiative and nonradiative rate constants for the TICT processes can be calculated from the observed values of fluorescence quantum yields, φ_f and lifetimes using the following Eqs. (5) and (6), which is more important in supporting and for explaining the above observation:

$$k_r = \frac{\varphi_f}{\tau} \tag{5}$$

$$k_{nr} = \frac{1}{\tau} - k_r \tag{6}$$

where τ, φ_f, k_r and k_{nr} are singlet state lifetime, fluorescence quantum yield, radiative and nonradiative rate constants, respectively. All these photophysical parameters are tabulated in Table 1. It is apparent from Table 1 that nonradiative rate constants, k_{nr} are decreased with increasing concentration of β-CD. Therefore, the enhanced lifetime is attributable to a reduction in the nonradiative rates.

However, very low lifetime value (187 ps) even at high concentration (9 mM) of β-CD molecules those actually have taken part in supramolecular assemblies through the formation of nanotubes indicates the possibility of quite a free movement of guest molecules inside the nanoscale channels formed by β-CD molecules. The complexation efficiency of guests with cyclodextrins is determined by relatively weak interactions, such as van der Waals forces, dipole–dipole and hydrogen bonding interactions [53,54]. The $-N(CH_3)_2$ group of DMASBT is unable to form hydrogen bonds with the hydroxyl groups present around the rims of a β-CD molecule. The weak van der Waals forces and dipole–dipole interactions operating inside the nanochannels are not enough for the total restriction of the movements of the guest molecules. Of course movements inside the nanotubes will be much more restricted than that in bulk aqueous medium which is reflected by the higher values of fluorescence anisotropy and lifetime at higher concentration of β-CD. Definitely a low lifetime because of the high rate of nonradiative processes towards triplet state cannot be ruled out. As mentioned above, the micropolarity of environment around DMASBT (5 μM) in nanotubes is similar to a medium having polarity in between ethanol and methanol. In a medium of this polarity, although TICT state of DMASBT is not so stabilized because enhanced fluorescence quantum yield is observed compared to the quantum yield of fluorescence from a highly stabilized TICT state in a medium of higher polarity like water, but still the energy state is expected to be quite close to the triplet state [42] resulting in the opening of nonradiative pathways and thereby reducing the lifetime of TICT state to a large extent. The increase in lifetime

Table 1
Excited singlet state lifetimes (τ), fluorescence quantum yields (ϕ), radiative (k_r) and nonradiative (k_{nr}) rate constants, steady state fluorescence anisotropies (r) and rotational correlation times (τ_c) of DMASBT in different concentrations of β-CD.

[β-CD] (mM)	τ (ps)[a]	χ^2	ϕ[b]	k_r (s^{-1})	k_{nr} (s^{-1})	r[a]	τ_c (ps)
5.0	135 ± 5	1.16	0.15 ± 0.001	1.11×10^9	6.30×10^9	0.28 ± 0.001	378 ± 5
7.0	158 ± 5	1.10	0.17 ± 0.001	1.08×10^9	5.25×10^9	0.29 ± 0.001	509 ± 5
9.0	187 ± 5	1.11	0.19 ± 0.001	1.02×10^9	4.33×10^9	0.31 ± 0.001	828 ± 5

[a] λ_{ex} = 370 nm, λ_{em} = 515 nm, and [DMASBT] = 5 μM.
[b] λ_{ex} = 370 nm and [DMASBT] = 5 μM.

with increasing concentration of β-CD is also in support to this statement.

The lifetime of DMASBT in glycerol is 830 ps which is much greater than that in β-CD [45]. As mentioned above the micropolarity of DMASBT lies in between ethanol and methanol. Since polarity of glycerol is not much different from that of methanol or ethanol, therefore it is expected that lower lifetime of DMASBT in β-CD cavity is due to the microenvironment with viscosity lower than the viscosity of pure glycerol. As a matter of fact, calculated microenvironment (68 cP) is in accordance with the observed low excited state lifetime of DMASBT in β-CD cavity. As for information, the viscosity of pure glycerol is 934 cP. This can also be supported by the fluorescence anisotropy value of 5 μM DMASBT in 9 mM β-CD which is 0.31 much different from the anisotropy in glycerol, i.e. 0.38. This is also attributable to the possibility of quite a large degree of reorientation of DMASBT molecules inside the tubes during the lifetime of its excited state which may further lead to assume that DMASBT is quite movable inside the nanotubes. Although the tumbling motion would be restricted inside the tubes causing high anisotropy, but motions along the tube and about the molecular axis are quite possible. This insists us to guess that only one molecule of DMASBT is included per β-CD molecule otherwise movements would have been much more restricted giving greater lifetime as observed in case of DMASBT in γ-CD (manuscript under preparation). This observation may also rule out that DMASBT molecules are not partially overlapped with one another inside the tubes [1].

It is well known that fluorescence anisotropy may change due to rotational diffusion of the molecule as well as the fluorescence lifetime. To make sure that the observed change in steady state anisotropy of DMASBT in different concentrations of β-CD is not due to any change in the fluorescence lifetime, Perrin's equation [43] (Eq. (7)) has been used to calculate the approximate values of the average rotational correlation times:

$$\tau_c = \frac{\tau \times r}{r_o - r} \tag{7}$$

where, r, r_o and τ are the steady state anisotropy, limiting anisotropy and lifetime of DMASBT, respectively. As mentioned above, the calculated values are approximate because of the unavailability of exact value of r_o as the time-resolved anisotropy could not be done. In the present calculation, the value of r_o is taken as 0.38 which is the anisotropy value of DMASBT in pure glycerol approximating that the limiting viscosity inside the nanotubes of β-CD will be similar to the viscosity of pure glycerol. Although the exact values of τ_c are not found, but at least the correct trend of the same is expected. The values of τ_c in the medium of different concentrations of β-CD calculated using Eq. (7) are also included in Table 1. The increase of τ_c with increasing concentration of β-CD definitely suggests that the observed changes in steady state fluorescence anisotropy values with 5 μM concentration of DMASBT (Fig. 3) are not due to lifetime induced phenomena but as predicted earlier that rotational restriction imposed on the molecule increases after inclusion in β-CD cavity and that further increases with increasing the concentration of β-CD.

4.. Conclusion

The formation of nanotubes of β-CD molecules is induced by guest molecule. Hydrophobic interactions between β-CD and guest molecules and hydrogen bonding interactions between neighboring β-CD molecules are essential for nanotube formation. Nanotubes further undergo secondary assembly through intertubular hydrogen bondings forming rod-like structures. The extent of nanotube formation and degree of their secondary assembly depend on the concentration of guest molecule. The critical aggregation concentration of DMASBT filled β-CD is found to be close to 2.5 mM. Guest molecules are quite movable inside the nanotubes. Although tumbling motions of guest molecules are restricted inside the tube but movements along the tubes are possible which do not favor the overlapping of guest molecules inside the tube suggesting that inclusion of one rather than two or more guest molecules per β-CD molecule. The supramolecular structures are possibly unstable in presence of high concentration of salting-in agent like sodium perchlorate. However, at low concentration of perchlorate ions (<7 mM) stability of supramolecular structures is increased because of the stronger hydrogen bonding interactions between neighboring β-CD molecules through ClO_4^- ions which provide anchor sites for hydrogen bondings. Micropolarity of environment around guest molecules inside nanotubes decreases whereas microviscosity increases with increasing concentration of guest molecule in the same concentration of β-CD. With high concentration of guest molecules, micropolarity of environment around guest molecule inside nanotubes formed by 10 mM concentration of β-CD is 54.5 which lie in between the polarities of methanol and ethanol. The microviscosity of the environment with 9 mM β-CD is 68 cP which is similar to the 82/18 (w/w) glycerol/water mixture.

Acknowledgements

SKS acknowledges University Grants Commission for financial supports under major research project (33-257/2007(SR)) and special assistance programme (F.540/14/DRS/2007 (SAP-I) and Council of Scientific and Industrial Research for financial supports under major research project (01(2213)/08/EMR-11), Govt. of India and PP acknowledges Department of Science and Technology, Govt. of India (SR/FTP/CS-114/2005). The authors also extend their acknowledgement to Professor Nitin Chattopadhyay of the Department of Chemistry, Jadavpur University, Calcutta, India for allowing them to use the time-resolved fluorescence set-up and Mr. G. Eranna and Mr. A. K. Sharma of Sensors and Microsystems Group, CEERI, Pilani 333031, Rajasthan, India for providing AFM facility and Mr. Mallari A. Naik for his help in taking TEM images.

Appendix A. Supplementary data

Supplementary data associated with this article can be found, in the online version, at doi:10.1016/j.jphotochem.2009.05.002.

References

[1] G. Li, L.B. McGown, Science 264 (1994) 249.
[2] G. Pistolis, A. Malliaris, J. Phys. Chem. 100 (1996) 15562.
[3] A. Wu, X. Shen, Y. He, J. Colloids Interface Sci. 297 (2006) 525.
[4] A. Wu, X. Shen, Y. He, J. Colloids Interface Sci. 302 (2006) 87.
[5] T.E. Girardeau, J. Leisen, H.W. Beckham, Macromol. Chem. Phys. 206 (2005) 998.
[6] R.A. Agbaria, D. Gill, J. Photochem. Photobiol. A: Chem. 78 (1994) 161.
[7] A.A. Rezik, D. David, J. Phys. Chem. 92 (1988) 1052.
[8] A.A. Kimberly, D.M. Tracy, A.A. Rezik, M.W. Isiah, J. Photochem. Photobiol. A: Chem. 91 (1995) 205.
[9] C. Zhang, X. Shen, H. Gao, Chem. Phys. Lett. 363 (2002) 515.
[10] P. Das, A. Chakrabarty, B. Haldar, A. Mallick, N. Chattopadhyay, J. Phys. Chem. B 111 (2007) 7401.
[11] L. Tormo, J.A. Organero, A. Douhal, J. Phys. Chem. B 109 (2005) 17848.
[12] M. El-Kemary, J.A. Organero, L. Santos, A. Douhal, J. Phys. Chem. B 110 (2006) 14128.
[13] A. Douhal, Chem. Rev. 104 (2004) 1955.
[14] T. Shimomura, T. Akai, T. Abe, K. Ito, J. Chem. Phys. 116 (2002) 1753.
[15] R. Isnin, A.E. Kaifer, J. Am. Chem. Soc. 113 (1992) 3136.
[16] A. Harada, J. Li, M. Kamachi, Nature 356 (1992) 325.
[17] A. Luttringhaus, F. Cramer, H. Prinzbach, Angew. Chem. 69 (1957) 137.
[18] B.J. Ravoo, R. Darcy, A. Mazzaglia, D. Nolan, K. Gaffney, Chem. Commun. (2001) 827.
[19] A. Harada, J. Li, M. Kamachi, Nature 364 (1993) 516.
[20] R. Breslow, S.D. Dong, Chem. Rev. 98 (1998) 1997.
[21] J.D. Badjic, V. Balzani, A. Credi, S. Silvi, J.F. Stoddart, Science 303 (2004) 1845.
[22] P. Mobian, J.-M. Kern, J.-P. Sauvage, J. Am. Chem. Soc. 125 (2003) 2016.
[23] P. Mobian, J.-M. Kern, J.-P. Sauvage, Angew. Chem. Int. Ed. Engl. 43 (2004) 2392.
[24] S.K. Saha, A.K. Kanchanmala, J. Surf. Sci. Technol. 22 (2006) 35.

[25] M. Christoff, L.T. Okano, C. Bohne, J. Photochem. Photobiol. A: Chem. 134 (2000) 169.
[26] B. Klingert, G. Rihs, Organometallics 9 (1990) 1135.
[27] N. Sarkar, K. Das, D. Nath, K. Bhattacharyya, Chem. Phys. Lett. 218 (1994) 492.
[28] O.S. Tee, M. Bozzi, J. Am. Chem. Soc. 112 (1990) 7815.
[29] H.J. Schneider, N.K. Sangwan, Angew. Chem. Int. Ed. Engl. 26 (1987) 896.
[30] K. Miyajima, M. Saweda, M. Nagakari, Bull. Chem. Soc. Jpn. 56 (1983) 3556.
[31] A.W. Coleman, I. Nicolis, N. Keller, J.P. Dalbiez, J. Incl. Phenom. Mol. Recognit. Chem. 13 (1992) 139.
[32] L. Szente, J. Szejtli, G.L. Kis, J. Pharm. Sci. 87 (1998) 778.
[33] G.G. Gaitano, P. Rodriguez, J.R. Isasi, M. Fuentes, G. Tardajos, M. Sanchez, J. Incl. Phenom. Macrocyc. Chem. 44 (2002) 101.
[34] P.J. Wright, C. Bohne, Can. J. Chem. 83 (2005) 1440.
[35] M. Bonini, S. Rossi, G. Karlsson, M. Almgren, P. Lo Nostro, P. Baglioni, Langmuir 22 (2006) 1478.
[36] S. Rossi, M. Bonini, P. Lo Nostro, P. Baglioni, Langmuir 23 (2007) 10959.
[37] S.S. Jaffer, S.K. Saha, G. Eranna, A.K. Sharma, P. Purkayastha, J. Phys. Chem. C 112 (2008) 11199.
[38] F.A. Long, W.F. McDevit, Chem. Rev. 52 (1952) 119.
[39] J.E. Gordon, The Organic Chemistry of Electrolyte Solutions, Wiley, New York, 1975.
[40] D.B. Wetlaufer, S.K. Malik, S. Stoller, R.L. Coffin, J. Am. Chem. Soc. 86 (1964) 508.
[41] J.K. Dey, E.L. Roberts, I.M. Warner, J. Phys. Chem. A 102 (1998) 301.
[42] S.K. Saha, P. Purkayastha, A.B. Das, J. Photochem. Photobiol. A: Chem. 195 (2008) 368.
[43] J.R. Lakowicz, Principles of Fluorescence Spectroscopy, Kluwer Academic/Plenum Publishers, New York, 1999.
[44] A.-B. Gorse, M. Pesquer, J. Phys. Chem. 99 (1995) 4039.
[45] S.K. Saha, P. Purkayastha, A.B. Das, S. Dhara, J. Photochem. Photobiol. A: Chem. 199 (2008) 179.
[46] P. Avouris, W.M. Gelbert, M.A. El-Sayed, Chem. Rev. 77 (1977) 793.
[47] R. Das, D. Guha, S. Mitra, S. Kar, S. Lahiri, S. Mukherjee, J. Phys. Chem. A 101 (1997) 4042.
[48] A. Mallick, B. Haldar, S. Maiti, N. Chattopadhyay, J. Colloids Interface Sci. 278 (2004) 215.
[49] A. Mallick, B. Haldar, N. Chattopadhyay, J. Phys. Chem. B 109 (2005) 14683.
[50] H.A. Benesi, J.H. Hildebrand, J. Am. Chem. Soc. 71 (1949) 2703.
[51] J. Szejtli, Chem. Rev. 98 (1998) 1743.
[52] R.P. Rohrbach, L.J. Rodriguez, E.M. Eyring, J. Phys. Chem. 81 (1977) 944.
[53] J. Szejtli, Cyclodextrins and Their Inclusion Complexes, Akademiai Kiado, Budapest, 1982, p. 142 and references therein.
[54] H.-J. Schneider, Angew. Chem. Int. Ed. Engl. 30 (1991) 1417.
[55] S.S. Jaffer, M. Sowmiya, S.K. Saha, P. Purkayastha, J. Colloids Interface Sci. 325 (2008) 236.
[56] R.B. Macgregor, G. Weber, Nature 319 (1986) 70.
[57] S.M. Dennison, J. Guharay, P.K. Sengupta, Spectrochim. Acta A 55 (1999) 1127.
[58] A. Sytnik, M. Kasha, Proc. Natl. Acad. Sci. U.S.A. 91 (1994) 8627.
[59] C. Reichardt, in: H. Ratajazak, W.J. Orville-Thomas (Eds.), Molecular Interaction, vol. 3, Wiley, New York, 1982, p. 255.
[60] E.M. Kossower, H. Doudik, K. Tanizawa, M. Ottoleghi, N. Orbach, J. Am. Chem. Soc. 97 (1975) 2167.
[61] A. Heredia, G. Requena, F.G. Sanchez, Chem. Commun. (1984) 1814.
[62] A. Szafranek, J. Szafranek, J. Incl. Phenom. Mol. Recognit. Chem. 30 (1998) 163.
[63] H. Yang, C. Bohne, J. Phys. Chem. 100 (1996) 14533.
[64] A. Mallick, B. Haldar, S. Maiti, S.C. Bera, N. Chattopadhyay, J. Phys. Chem. B 109 (2005) 14675.
[65] X. Wang, J. Wang, Y. Wang, H. Yan, P. Li, R.K. Thomas, Langmuir 20 (2004) 53.
[66] F.G. Prendergast, Curr. Opin. Struct. Biol. 1 (1991) 1054.
[67] A. Chattopadhyay, S. Mukherjee, H. Raghuraman, J. Phys. Chem. B 106 (2002) 13002.
[68] N. Sarkar, A. Datta, S. Das, K. Bhattacharyya, J. Phys. Chem. 100 (1996) 15483.